Parameter Optimization of Biochemical Models for Precision Medicine: A Case Study in PI(4,5)P_2 Synthesis

Gonzalo Hernandez-Hernandez*[1,2], Mindy Tieu[2], Pei-Chi Yang[1,2], L. Fernando Santana[2] and Colleen E. Clancy*[1,2,3]

[1]*Center for Precision Medicine and Data Science,*
[2]*Department of Physiology and Membrane Biology,*
[3]*Department of Pharmacology,*
University of California, Davis, California

*Corresponding authors
Email: ghernandezh@ucdavis.edu, ceclancy@ucdavis.edu

Short title: PIP_2 Modeling for Precision Biomedicine

Author Contributions: G.H.H. and PC.Y. designed the research study, conducted simulations, acquired data, analyzed data, and wrote the manuscript. M.T., L.F.S. and C.E.C analyzed data, and wrote the manuscript.

Competing Interest Statement: The authors declare no competing interests.

Classification: Biological Sciences, Biophysics and Computational Biology

Keywords: Phosphoinositide Metabolism, Parameter Estimation, Precision Lipid Signaling Models

Abstract

Lipidomics is emerging as a domain of opportunity for precision medicine, with phosphatidylinositol 4,5-bisphosphate (PI(4,5)P_2) functioning as a central regulator of membrane signaling and metabolic control. Its rapid turnover and involvement in diseases like cancer and neurodegeneration highlight its dual role as a biomarker and therapeutic target. However, the inherent complexity of lipid networks complicates traditional modeling approaches. We present a modular, extendable framework for constructing mechanistic models of lipid kinetics via a case study, modeling the synthesis and degradation of phosphatidylinositol 4,5-bisphosphate (PI(4,5)P_2), a second messenger central to receptor signaling and calcium regulation. Our method efficiently identifies rate constants governing enzymatic dynamics and can be extended to a range of signaling networks. Using experimental time-course data for PI(4)P, PI(4,5)P_2, and IP_3, we optimized five kinetic parameters to capture the lipid and second messenger dynamics. The resulting model achieved a strong correlation with experimental trends and reproduced dynamic behaviors relevant to cellular signaling. We then applied the model to simulate signaling perturbations linked to *PI4KA* and *PIP5K1C* loss-of-function, two lipid kinases associated with neurodevelopmental and neuromuscular disorders. This modeling framework provides a scalable foundation for predictive biochemical modeling and offers a path toward individualized applications in precision medicine.

Introduction

Precision medicine seeks to personalize treatment by accounting for individual variation in genes, environment, and lifestyle that traditional methods have overlooked. Bridging this gap requires not only richer data but also flexible, dynamic models that reflect the complexity of human biology. In rare diseases, next-generation sequencing often yields variants of unknown significance that lack clear functional interpretation, limiting diagnosis and preventing targeted treatment. This gap is particularly critical in lipid signaling disorders, where the nonlinear behavior and chemical diversity of lipid intermediates prevent direct mechanistic interpretation without dynamic modeling frameworks (Zandl-Lang et al., 2023).

Lipidomics represents a critical frontier for precision medicine. Phosphatidylinositol 4,5-bisphosphate ($PI(4,5)P_2$) is fundamental to precision medicine because it serves as the master regulator in cellular signaling, membrane dynamics, and metabolism that vary across individuals (Balla, 2013; Viaud et al., 2016). Lipids play important roles in diseases such as cancer, neurodegeneration, and metabolic disorders that make them valuable biomarkers and therapeutic targets (Burke et al., 2023). However, the practical study of lipids requires sophisticated tools and multidisciplinary strategies due to the diversity, transient nature, and complexity of lipid measurements.

$PI(4,5)P_2$ plays a primary role in plasma membrane signaling. Sequential phosphorylation of phosphatidylinositol (PI) to PI(4)P and then to $PI(4,5)P_2$, catalyzed by PI 4-kinase (PI4K) and PI(4)P 5-kinase (PIP5K), respectively, drives $PI(4,5)P_2$ synthesis. Intermediates formed during this process regulate cellular processes that include vesicle trafficking, cytoskeletal remodeling, and receptor signaling (De Camilli et al., 1996; Di Paolo et al., 2004). Hydrolysis of $PI(4,5)P_2$ by phospholipase C (PLC) forms diacylglycerol (DAG) and inositol trisphosphate (IP_3), two second messengers that propagate downstream responses (Berridge, 1993, 2009; Berridge & Irvine, 1984, 1989). Rapid turnover and nonlinear feedback regulation of intermediates create a dynamic landscape that challenges traditional prediction techniques. Mechanistic modeling of these dynamics offers an opportunity to link kinase dysfunction to disease-relevant alterations in lipid signaling behavior.

Mathematical modeling and simulation are indispensable tools for predicting lipid dynamics, enabling the quantitative representation of biochemical networks and the prediction of system behavior under various perturbations. However, existing modeling strategies also face persistent challenges, including extraction of reliable kinetic rate constants, as direct measurements can be difficult or impossible with current experimental and clinical approaches. Here, we introduce a modular and extendable modeling framework for constructing and refining lipid kinetic models using a minimal set of ordinary differential equations (ODEs) in conjunction with nonlinear parameter optimization based on the Nelder–Mead algorithm (Hernandez-Hernandez et al., 2024; Kernik et al., 2019; Moreno et al., 2016).

We applied a multi-start Nelder–Mead algorithm to refine a kinetic model of $PI(4,5)P_2$ synthesis and degradation using experimental data from superior cervical ganglion (SCG) neurons (Kruse et al., 2016). The optimization approach combines convergence efficiency with the flexibility to incorporate biological constraints and experimental insight. The optimized model captures dynamic lipid responses to muscarinic receptor stimulation (Dickson et al., 2013; Falkenburger et al., 2010; Kruse et al., 2016). To evaluate the capacity of the model to simulate disease-relevant signaling outcomes, the simulations target two lipid kinases, PI4KA and PIP5K1C, which regulate sequential steps in $PI(4,5)P_2$ production and are implicated

in neurodevelopmental and neuromuscular disorders (Burke et al., 2023; Narkis et al., 2007; Salter et al., 2021; Verdura et al., 2021). Simulation results derived from dynamic model behavior reveal functional consequences of enzyme-specific perturbations and support the development of data-driven, individualized modeling strategies for disease-linked biochemical processes. This method offers a computationally efficient and adaptable approach for refining parameters across diverse biochemical systems.

Methods

A system of differential equations was used to represent the dynamic interconversion of phosphatidylinositol (PI), phosphatidylinositol 4-phosphate (PI(4)P), and phosphatidylinositol 4,5-bisphosphate ($PI(4,5)P_2$), as well as the hydrolytic cleavage of $PI(4,5)P_2$ by phospholipase C (PLC), yielding inositol trisphosphate (IP_3) and diacylglycerol (DAG). The model is depicted in **Figure 1A**.

Assuming a 1 pL spherical cell with a membrane area of 480 μm^2 and 3000 PIP molecules/μm^2, we calculated a concentration of 0.00239 mM. Initial lipid ratios follow mass spectrometry data (Kruse et al., 2016): $PI:PI(4)P:PI(4,5)P_2 = 100:1:1.713$. Given the abundance and slow turnover of PI, it was treated as a constant reservoir via a steady-state approximation:

$$\frac{d[PI]}{dt} = 0 \tag{1}$$

The concentration of PI(4)P changes through multiple reactions. PI is phosphorylated by PI4K to form PI(4)P, while PI(4)P undergoes dephosphorylation back to PI. To preserve a cellular ratio of approximately 100:1 between PI and PI(4)P, the reverse rate is scaled accordingly. PI(4)P also acts as a precursor for $PI(4,5)P_2$ through the action of PIP5K, and is regenerated from $PI(4,5)P_2$ by a 5-phosphatase reaction modulated by a nonlinear feedback term. These contributions yield the following expression:

$$\frac{d[PI(4)P]}{dt} = k_{PI4K}[PI] + k_{5P} * f_1[PI(4,5)P_2] - k_{4P}[PI(4)P] - k_{PIP5K}[PI(4)P] \tag{2}$$

To preserve the ~100-fold excess of PI relative to PI(4)P, the dephosphorylation rate constant k_{4P} is defined as $k_{4P} = k_{PI4K} * 100$. The feedback function f_1, which modulates the activity of the 5-phosphatase, is dependent on the concentration of $PI(4,5)P_2$ and incorporates saturation kinetics through a Hill function:

$$f_1 = \frac{[PI(4,5)P_2]^n}{k^n + [PI(4,5)P_2]^n}, n = 2.5, k = 0.3 \tag{3}$$

The effective activity of the 5-phosphatase is then defined as:

$$k_{Eff} = k_{5P} * f_1 \tag{4}$$

The concentration of $PI(4,5)P_2$ is governed by the rate of its formation from PI(4)P and its consumption through cleavage by activated PLC (denoted PLC_1). Additionally, the degradation of IP_3 contributes to overall depletion of $PI(4,5)P_2$ via mass redistribution. This leads to the following governing equation:

$$\frac{d[PI(4,5)P_2]}{dt} = \mathrm{k_{PIP5K}}[PI(4)P] - k_{PLC}[PI(4,5)P_2] * PLC_1 - k_{deg}[IP_3] \quad (5)$$

IP_3 production and degradation are described by a balance between synthesis through PLC-mediated hydrolysis of $PI(4,5)P_2$ and degradation through independent enzymatic action. The resulting rate equation is:

$$\frac{d[IP_3]}{dt} = \mathrm{k_{PLC}}[PI(4,5)P_2] * PLC_1 - k_{deg}[IP_3] \quad (6)$$

Altogether, five kinetic parameters with units of s^{-1}, namely, kPI_{4K}, k_{PIP5K}, k_{5P}, k_{PLC}, *and* k_{deg} govern the dynamic behavior of the system.

Parameter Optimization of the Phosphoinositide Signaling Model

The Nelder-Mead method was employed to estimate the kinetic parameters that govern the time-dependent behavior of phosphoinositide intermediates, including PI(4)P, $PI(4,5)P_2$, and IP_3. The system comprises five parameters (k_{PI4K}, k_{PIP5K}, k_{5P}, k_{PLC}, k_{deg}) that represent enzymatic synthesis, phosphorylation, dephosphorylation, hydrolysis, and degradation processes within the signaling network. Optimization minimized the difference between the model and experimental recorded time-series data, normalized to the peak amplitude of each dataset.

The cost function was defined as the total sum of squared errors (SSE) across all time points:

$$\mathrm{SSE} = \sum_{\mathrm{i=1}}^{\mathrm{n}}[\left(PIP_i^{model} - PIP_i^{data}\right)^2 + \left(PIP2_i^{model} - PIP2_i^{data}\right)^2 + \left(IP3_i^{model} - IP3_i^{data}\right)^2] \quad (7)$$

The Nelder–Mead algorithm is a derivative-free direct search method and modifies a set of candidate solutions through reflection, expansion, contraction, and shrinkage. A bounded transformation confined all parameters to the biologically plausible range of 10^{-8} to 5000.

To mitigate the risk of convergence to local minima, a multi-start global optimization strategy was employed. Each trial was initialized with a randomly generated parameter vector. Upon identifying a local minimum, the parameters were perturbed by independently perturbing each value within ±20%, and the resulting vector was used to initiate a new optimization run. This process was repeated for 1,000 independent trials. The parameter set yielding the lowest total sum of squared errors (SSE) across all iterations was selected as the optimal solution.

Model accuracy was assessed through residual diagnostics. Metrics included the sum of squared errors, the standard mean error, as well as error decomposition by molecular species. The proposed framework, which combines Nelder–Mead optimization with a stochastic global search, proved to be robust and flexible.

Results

The model schematic representing the dynamic interconversion of phosphatidylinositol (PI), phosphatidylinositol 4-phosphate (PI(4)P), and phosphatidylinositol 4,5-bisphosphate ($PI(4,5)P_2$), as well as the hydrolytic cleavage of $PI(4,5)P_2$ by phospholipase C (PLC), yielding inositol trisphosphate (IP_3) and diacylglycerol (DAG), is shown in **Figure 1A**. **Figure 1B** shows the differential equations in the model for phosphoinositide intermediates (PI(4)P, $PI(4,5)P_2$, and IP_3) on the left and five kinetic parameters subject to parameter optimization on the right.

In superior cervical ganglion (SCG) neurons, the application of 10 μM Oxo-M for 20 seconds activates muscarinic (M1) receptors, leading to PI(4)P and $PI(4,5)P_2$ depletion through PLC-mediated hydrolysis (Kruse et al., 2016). Assuming a readily available pool of PI in SCG neurons, we applied parameter optimization using the Nelder–Mead algorithm to fit the model to experimental time course of PI(4)P, $PI(4,5)P_2$, and IP_3 in response to PLC application and then extracted the five enzymatic kinetic parameters. The optimized model accurately recapitulated the dynamic depletion and recovery of $PI(4,5)P_2$ as well as the generation of IP_3 in response to stimulation. This is indicated by the optimization yielding close agreement with experimentally measured concentrations of PI(4)P, $PI(4,5)P_2$, and IP_3 (**Figure 1C, i, ii, and iii,** respectively), confirming that the model structure is sufficient to recapitulate key features of lipid signaling kinetics. The fit quality is supported by low mean squared error values: 0.0148 for PI(4)P, 0.0033 for $PI(4,5)P_2$, and 0.0015 for IP_3.

To demonstrate the potential application of the optimized model of $PI(4,5)P_2$ lipid dynamics in precision medicine, we performed predictive simulations targeting signaling outcomes considering genetic or pharmacologic perturbations relevant to neurodegenerative disease. Disruption in phosphoinositide metabolism is foundational in disease states, offering opportunities to unravel lipid kinase activity mechanisms. The simulations specifically examined loss-of-function mutations in *PI4KA* and *PIP5KIC*. The perturbations were implemented by reducing the rate constants k_{PI4K} and k_{PIP5K}, which describe the enzymatic activity of PI4K and PIP5K (**Figure D–F**).

To evaluate the consequences of PI4KA dysfunction on phosphoinositide signaling, we simulated lipid and IP_3 responses during repeated 20-second receptor stimulation delivered every 300 seconds. PI4KA encodes the brain-enriched lipid kinase PI4KIIIα, which forms a ternary complex with TTC7 and FAM126 that stabilizes and activates the catalytic function of the enzyme (Nakatsu et al., 2012; Suresh et al., 2024). Loss-of-function mutations in this complex reduce enzymatic activity and result in neurological disorders (Salter et al., 2021; Verdura et al., 2021). To reproduce these conditions, we reduced PI4K activity by 60% and 90%, consistent with reported levels of pharmacological inhibition (Bojjireddy et al., 2014). The simulations revealed progressive depletion of PI(4)P (**Figure D-i**), followed by substantial reductions in $PI(4,5)P_2$ (**Figure D-ii**) and IP_3 signaling (**Figure D-iii**) with delayed recovery between stimulation pulses. The reduction in $PI(4,5)P_2$ and attenuation of calcium-linked IP_3 production are consistent with molecular features reported in PI4KA-associated disease, supporting the capacity of the model to establish mechanistic links between kinase loss and disrupted phosphoinositide signaling.

$PI(4,5)P_2$ synthesis primarily relies on PIP5K activity. The pathway includes three isoforms: PIP5KIα, PIP5KIβ, and PIP5KIγ. PIP5KIγ localizes to the plasma membrane and is essential for synaptic transmission and synaptic vesicle trafficking. Loss-of-function mutations in PIP5KIγ (PIP5K1C, MIM: 606102) are associated with reduced $PI(4,5)P_2$ levels and cause lethal congenital contractural syndrome 3

(Morleo et al., 2023; Narkis et al., 2007). To examine the impact of PIP5K dysfunction, we applied 60% and 90% reductions in the rate constant kPIP5K. The simulations employed the same protocol used previously, repeated 20-second receptor stimulations delivered every 300 seconds. The model predicted disruptions in PI(4)P availability (**Figure E-i**) and impaired PI(4,5)P_2 synthesis (**Figure E-ii**), while IP_3 production remained largely unaffected (**Figure E-iii**). These predictions align with clinical and experimental findings showing that PIP5K1C mutations cause reduced PI(4,5)P_2 levels and synaptic dysfunction without broad second messenger impairment (Di Paolo et al., 2004).

Combined loss-of-function in *PI4KA* and *PIP5K1C* has not been documented in clinical reports, possibly due to lethality. However, simulation of this condition allowed dissection of the compound effects under the same repeated stimulation protocol. Dual inhibition of PI4K and PIP5K produced severe and synergistic defects, depleting PI(4)P (**Figure F-i**) and PI(4,5)P_2 (**Figure F-ii**), and damping of IP_3 oscillations (**Figure F-iii**). The results demonstrate that PI4K governs the availability of upstream precursors, whereas PIP5K controls the terminal conversion. When both enzymes are impaired, the resulting amplification of lipid depletion disrupts the entire signaling cascade.

The model predictions from a mechanistic model framework allow for interpreting enzyme-specific vulnerabilities in phosphoinositide signaling and establish the model as a predictive platform for precision analysis of disease-associated perturbations.

Discussion

The optimized model presented here recapitulates key features of phosphoinositide signaling, capturing the dynamic interplay between PI(4)P, PI(4,5)P_2, and IP_3 with high fidelity. The good fits in optimization to time-resolved experimental data under defined receptor stimulation establishes a robust foundation for investigating lipid kinase function under perturbed conditions and can be generalized to biochemical networks produced by the activation of G-protein-coupled receptors. Importantly, this model advances precision medicine by connecting dynamic lipid kinetics to enzyme-specific alterations underlying individual disease profiles, enabling simulation-based predictions of pathological signaling in rare or poorly characterized conditions.

The predictions from modeling and simulation suggest that PI4KA and PIP5K1C serve distinct yet interdependent functions in maintaining lipid pool homeostasis. PI4KA regulates PI(4)P availability upstream, whereas PIP5K1C controls the final enzymatic step in PI(4,5)P_2 synthesis. Perturbation of PI4KA or PIP5K1C produces unique alterations in lipid dynamics. However, combined inhibition results in a compounded signaling collapse not observed during individual enzymatic disruptions. The simulations in the study presented here focus on loss-of-function mutations. In contrast, PIP5K1C mutation can be also associated with gain-of-function, leading to abnormal IP_3 production under pathological conditions (Morleo et al., 2023). We performed such a simulation, and the model predicted uncontrolled production of IP_3, suggesting high Ca^{2+} concentration as a mechanism to disrupt cell signaling and even initiate cell death. The model outputs reveal critical inter-enzyme dependencies and suggest mechanisms through which disrupted phosphoinositide metabolism may impair cellular function in neurodevelopmental and neuromuscular disorders (Burke et al., 2023; Narkis et al., 2007; Salter et al., 2021; Verdura et al., 2021). The simulations reproduce known pathological phenotypes of PI4KA and PIP5K1C related diseases, while also providing plausible mechanistic predictions for genetic combinations that are likely to be embryonically lethal.

The modeling strategy introduced here invites the design of new experimental systems aimed at reinforcing model-derived predictions and expanding *in silico* analysis pipelines. A strength of the current framework is its foundation in time-resolved lipid measurements derived from the same cellular context. This level of internal consistency, exemplified by the elegant studies of Kruse et al., (Kruse et al., 2016) distinguishes the present approach from prior experimental studies that focused on either $PI(4,5)P_2$ or IP_3 production in isolation. The availability of aligned time courses for PI(4)P, $PI(4,5)P_2$, and IP_3 enables parameter optimization with better precision and enhances the biological interpretability of model outputs. Importantly, the integrated experimental-computational strategy developed in the present work establishes a novel platform for studying $PI(4,5)P_2$ signaling in specific biological contexts.

The computational framework supports simulation of signaling outcomes under biologically inaccessible or lethal conditions. For example, compound genotypes can be modeled to forecast lipid depletion profiles and second messenger dynamics during repeated stimulation. Consequently, the strategy extends beyond data fitting to enable hypothesis generation in systems not directly testable by experimental means. The framework offers a generalizable foundation for mechanistic inference, disease modeling, and targeted hypothesis development. Overall, the model provides a decisive step toward a mechanistically grounded and precision-oriented understanding of phosphoinositide dysfunction in lipid signaling disorders.

Simulations protocols

Code for simulations and analysis was written in MATLAB 2018b. The MATLAB optimization routine was run on an Apple Mac Pro machine with two 2.7 GHz 12-Core Intel Xeon processors and an HP ProLiant DL585 G7 server with a 2.7 GHz 28-core AMD Opteron processor. Numerical results were visualized using MATLAB R2018a by The MathWorks, Inc. All codes are available on GitHub (https://github.com/ClancyLabUCD/parameter-optimization-of-biochemical-models-for-precision-medicine-pip2)

Acknowledgments

This work was supported by National Heart, Lung, and Blood Institute grants 1R01HL174001 (C.E.C, L.F.S.,), R01HL168874 (C.E.C., L.F.S.). The UC Davis Chancellor's Postdoctoral Fellowship (G.H.H.) and the UC Davis Center for Precision Medicine and Data Sciences.

References

Balla, T. (2013). Phosphoinositides: Tiny lipids with giant impact on cell regulation. *Physiological Reviews*, *93*(3), 1019–1137. https://doi.org/10.1152/physrev.00028.2012

Berridge, M. J. (1993). Inositol trisphosphate and calcium signalling. *Nature*, *361*(6410), 315–325. https://doi.org/10.1038/361315a0

Berridge, M. J. (2009). Inositol trisphosphate and calcium signalling mechanisms. *Biochimica Et Biophysica Acta*, *1793*(6), 933–940. https://doi.org/10.1016/j.bbamcr.2008.10.005

Berridge, M. J., & Irvine, R. F. (1984). Inositol trisphosphate, a novel second messenger in cellular signal transduction. *Nature*, *312*(5992), 315–321. https://doi.org/10.1038/312315a0

Berridge, M. J., & Irvine, R. F. (1989). Inositol phosphates and cell signalling. *Nature*, *341*(6239), 197–205. https://doi.org/10.1038/341197a0

Bojjireddy, N., Botyanszki, J., Hammond, G., Creech, D., Peterson, R., Kemp, D. C., Snead, M., Brown, R., Morrison, A., Wilson, S., Harrison, S., Moore, C., & Balla, T. (2014). Pharmacological and Genetic Targeting of the PI4KA Enzyme Reveals Its Important Role in Maintaining Plasma Membrane Phosphatidylinositol 4-Phosphate and Phosphatidylinositol 4,5-Bisphosphate Levels. *Journal of Biological Chemistry*, *289*(9), 6120–6132. https://doi.org/10.1074/jbc.M113.531426

Burke, J. E., Triscott, J., Emerling, B. M., & Hammond, G. R. V. (2023). Beyond PI3Ks: Targeting phosphoinositide kinases in disease. *Nature Reviews Drug Discovery*, *22*(5), 357–386. https://doi.org/10.1038/s41573-022-00582-5

De Camilli, P., Emr, S. D., McPherson, P. S., & Novick, P. (1996). Phosphoinositides as Regulators in Membrane Traffic. *Science*, *271*(5255), 1533–1539. https://doi.org/10.1126/science.271.5255.1533

Di Paolo, G., Moskowitz, H. S., Gipson, K., Wenk, M. R., Voronov, S., Obayashi, M., Flavell, R., Fitzsimonds, R. M., Ryan, T. A., & Camilli, P. D. (2004). Impaired PtdIns(4,5)P2 synthesis in nerve terminals produces defects in synaptic vesicle trafficking. *Nature*, *431*(7007), 415–422. https://doi.org/10.1038/nature02896

Dickson, E. J., Falkenburger, B. H., & Hille, B. (2013). Quantitative properties and receptor reserve of the IP(3) and calcium branch of G(q)-coupled receptor signaling. *The Journal of General Physiology*, *141*(5), 521–535. https://doi.org/10.1085/jgp.201210886

Falkenburger, B. H., Jensen, J. B., & Hille, B. (2010). Kinetics of PIP2 metabolism and KCNQ2/3 channel regulation studied with a voltage-sensitive phosphatase in living cells. *Journal of General Physiology*, *135*(2), 99–114. https://doi.org/10.1085/jgp.200910345

Hernandez-Hernandez, G., O'Dwyer, S. C., Yang, P.-C., Matsumoto, C., Tieu, M., Fong, Z., Lewis, T. J., Santana, L. F., & Clancy, C. E. (2024). A computational model predicts sex-specific responses to calcium channel blockers in mammalian mesenteric vascular smooth muscle. *eLife*, *12*, RP90604. https://doi.org/10.7554/eLife.90604

Kernik, D. C., Morotti, S., Wu, H., Garg, P., Duff, H. J., Kurokawa, J., Jalife, J., Wu, J. C., Grandi, E., & Clancy, C. E. (2019). A computational model of induced pluripotent stem-cell derived cardiomyocytes incorporating experimental variability from multiple data sources. *The Journal of Physiology*, *597*(17), 4533–4564. https://doi.org/10.1113/JP277724

Kruse, M., Vivas, O., Traynor-Kaplan, A., & Hille, B. (2016). Dynamics of Phosphoinositide-Dependent Signaling in Sympathetic Neurons. *The Journal of Neuroscience*, *36*(4), 1386–1400. https://doi.org/10.1523/JNEUROSCI.3535-15.2016

398 Moreno, J. D., Lewis, T. J., & Clancy, C. E. (2016). Parameterization for In-Silico Modeling of Ion
399 Channel Interactions with Drugs. *PloS One*, *11*(3), e0150761.
400 https://doi.org/10.1371/journal.pone.0150761
401 Morleo, M., Venditti, R., Theodorou, E., Briere, L. C., Rosello, M., Tirozzi, A., Tammaro, R., Al-Badri,
402 N., High, F. A., Shi, J., Acosta, M. T., Adam, M., Adams, D. R., Alvarez, R. L., Alvey, J.,
403 Amendola, L., Andrews, A., Ashley, E. A., Bacino, C. A., … Franco, B. (2023). De novo
404 missense variants in phosphatidylinositol kinase PIP5KIγ underlie a neurodevelopmental
405 syndrome associated with altered phosphoinositide signaling. *The American Journal of Human*
406 *Genetics*, *110*(8), 1377–1393. https://doi.org/10.1016/j.ajhg.2023.06.012
407 Nakatsu, F., Baskin, J. M., Chung, J., Tanner, L. B., Shui, G., Lee, S. Y., Pirruccello, M., Hao, M.,
408 Ingolia, N. T., Wenk, M. R., & De Camilli, P. (2012). PtdIns4P synthesis by PI4KIIIα at the
409 plasma membrane and its impact on plasma membrane identity. *Journal of Cell Biology*, *199*(6),
410 1003–1016. https://doi.org/10.1083/jcb.201206095
411 Narkis, G., Ofir, R., Landau, D., Manor, E., Volokita, M., Hershkowitz, R., Elbedour, K., & Birk, O. S.
412 (2007). Lethal Contractural Syndrome Type 3 (LCCS3) Is Caused by a Mutation in *PIP5K1C,*
413 Which Encodes PIPKIγ of the Phophatidylinsitol Pathway. *The American Journal of Human*
414 *Genetics*, *81*(3), 530–539. https://doi.org/10.1086/520771
415 Salter, C. G., Cai, Y., Lo, B., Helman, G., Taylor, H., McCartney, A., Leslie, J. S., Accogli, A., Zara, F.,
416 Traverso, M., Fasham, J., Lees, J. A., Ferla, M. P., Chioza, B. A., Wenger, O., Scott, E., Cross,
417 H. E., Crawford, J., Warshawsky, I., … Baple, E. L. (2021). Biallelic PI4KA variants cause
418 neurological, intestinal and immunological disease. *Brain*, *144*(12), 3597–3610.
419 https://doi.org/10.1093/brain/awab313
420 Suresh, S., Shaw, A. L., Pemberton, J. G., Scott, M. K., Harris, N. J., Parson, M. A. H., Jenkins, M. L.,
421 Rohilla, P., Alvarez-Prats, A., Balla, T., Yip, C. K., & Burke, J. E. (2024). Molecular basis for
422 plasma membrane recruitment of PI4KA by EFR3. *Science Advances*, *10*(51), eadp6660.
423 https://doi.org/10.1126/sciadv.adp6660
424 Verdura, E., Rodríguez-Palmero, A., Vélez-Santamaria, V., Planas-Serra, L., de la Calle, I., Raspall-
425 Chaure, M., Roubertie, A., Benkirane, M., Saettini, F., Pavinato, L., Mandrile, G., O'Leary, M.,
426 O'Heir, E., Barredo, E., Chacón, A., Michaud, V., Goizet, C., Ruiz, M., Schlüter, A., … Pujol,
427 A. (2021). Biallelic PI4KA variants cause a novel neurodevelopmental syndrome with
428 hypomyelinating leukodystrophy. *Brain*, *144*(9), 2659–2669.
429 https://doi.org/10.1093/brain/awab124
430 Viaud, J., Mansour, R., Antkowiak, A., Mujalli, A., Valet, C., Chicanne, G., Xuereb, J.-M., Terrisse, A.-
431 D., Séverin, S., Gratacap, M.-P., Gaits-Iacovoni, F., & Payrastre, B. (2016). Phosphoinositides:
432 Important lipids in the coordination of cell dynamics. *Biochimie*, *125*, 250–258.
433 https://doi.org/10.1016/j.biochi.2015.09.005
434 Zandl-Lang, M., Plecko, B., & Köfeler, H. (2023). Lipidomics—Paving the Road towards Better Insight
435 and Precision Medicine in Rare Metabolic Diseases. *International Journal of Molecular*
436 *Sciences*, *24*(2), Article 2. https://doi.org/10.3390/ijms24021709
437

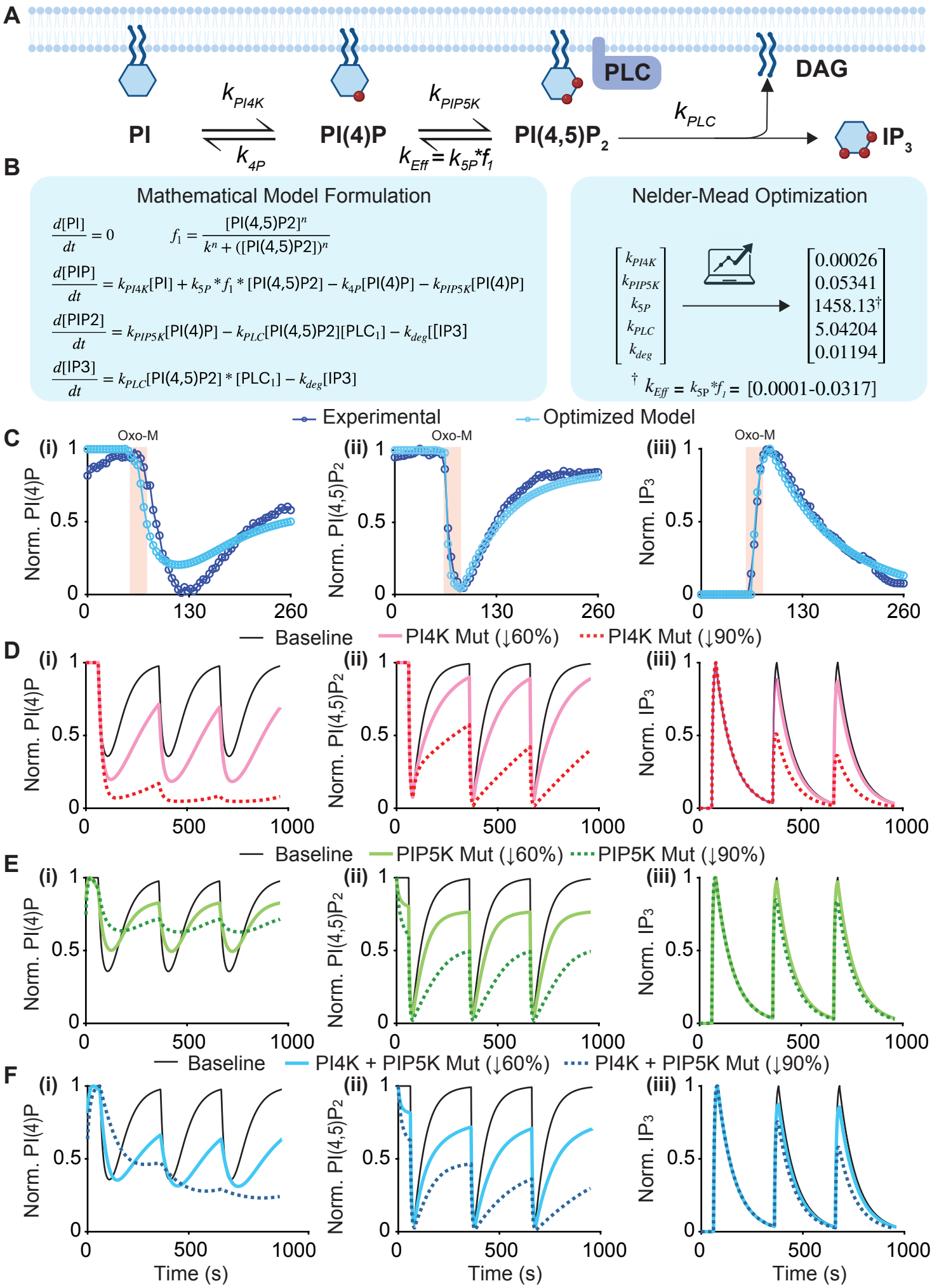
A
PLC
DAG
PI
PI(4)P
PI(4,5)P2
IP3
kPI4K
k4P
kPIP5K
kEff = k5P*f1
kPLC
B
Mathematical Model Formulation
Nelder-Mead Optimization
0.00026
0.05341
1458.13†
5.04204
0.01194
† kEff = k5P*f1 = [0.0001-0.0317]
Experimental
Optimized Model
C
Oxo-M
Norm. PI(4)P
Norm. PI(4,5)P2
Norm. IP3
D
Baseline
PI4K Mut (↓60%)
PI4K Mut (↓90%)
E
PIP5K Mut (↓60%)
PIP5K Mut (↓90%)
F
PI4K + PIP5K Mut (↓60%)
PI4K + PIP5K Mut (↓90%)
Time (s)

Figure 1. **A**) Phosphatidylinositol (PI) is sequentially phosphorylated by PI 4-kinase (PI4K) to form phosphatidylinositol 4-phosphate (PI(4)P), which is subject to dephosphorylation by 4-phosphatases (k_{4P}). PI(4)P is further phosphorylated by phosphatidylinositol 4-phosphate 5-kinase (PIP5K) to produce phosphatidylinositol 4,5-bisphosphate ($PI(4,5)P_2$), a central signaling lipid. This species can be dephosphorylated by 5-phosphatases (k_{5P}) or cleaved by PLC, yielding two key second messengers: membrane-bound diacylglycerol (DAG) and soluble inositol 1,4,5-trisphosphate (IP_3). **B**) *Left:* A system of differential equations models the reaction kinetics, incorporating a feedback function f1 modulated by $PI(4,5)P_2$ abundance. *Right:* Five parameters—k_{PI4K}, k_{PIP5K}, k_{5P}, k_{PLC}, and k_{deg}—were optimized against empirical data. **C**) Model fitting results of 20 seconds application of muscarinic agonist 10 μM Oxo-M (Kruse et al., 2016). Time-course plots of PI(4)P (i), $PI(4,5)P_2$ (ii), and IP_3 (iii) show close agreement between experimental data (dark blue circles) and optimized model predictions (light blue dots). **D**) Effects of PI4K mutation causing 60% and 90% reduction in k_{PI4K} under repeated PLC activation (20 s pulses every 300 s) leading to attenuated $PI(4,5)P_2$ and IP_3 responses. **E**) Effects of PIP5K mutation with 60% and 90% reduction in k_{PIP5K} of PI(4)P (i), $PI(4,5)P_2$ (ii), and IP_3 (iii). **F**) Combined 60% and 90% reductions PI4K and PIP5K revealing synergistic disruption of signaling of PI(4)P (i), $PI(4,5)P_2$ (ii), and IP_3 (iii).